

# We are IntechOpen, the world's leading publisher of Open Access books Built by scientists, for scientists

6,900

Open access books available

185,000

International authors and editors

200M

Downloads

Our authors are among the

154

Countries delivered to

TOP 1%

most cited scientists

12.2%

Contributors from top 500 universities



WEB OF SCIENCE™

Selection of our books indexed in the Book Citation Index  
in Web of Science™ Core Collection (BKCI)

Interested in publishing with us?  
Contact [book.department@intechopen.com](mailto:book.department@intechopen.com)

Numbers displayed above are based on latest data collected.  
For more information visit [www.intechopen.com](http://www.intechopen.com)



# Focused Ion Beam Tomography

*Dilawar Hassan, Sidra Amin, Amber Rehana Solangi  
and Saima Q. Memon*

## Abstract

To study the fundamental effect of shape and morphology of any material on its properties, it is very essential to know and study its morphology. Focused ion beam (FIB) tomography is a 3D chemical and structural relationship studying technique. The instrumentation of FIB looks like that of the scanning electron microscopy (SEM), but there is a major difference in the beam used for scanning. For SEM, a beam of electrons is used with scanning medium whereas in FIB, a much focused beam of ions is used for scanning. FIB can be used for lithography and ablation purposes, but due to advancements and high-energy focused beam, it is nowadays being used as a tomographic technique. Tomography is defined as imaging by sectioning or cross-sectioning any desired area. The hyphenation of FIB with energy-dispersive spectrometry or secondary ion mass spectrometry can give us elemental analysis with very high-resolution 3D images for a sample. This technique contributes to acquaintance of qualitative and quantitative analyses, 3D volume creations, and image processing. In this chapter, we will discuss the advancements in FIB instrumentation and its use as 3D imaging tool for different samples ranging from nanometer (nm)-sized materials to micrometer ( $\mu\text{m}$ )-sized biological samples.

**Keywords:** focused ion beam, scanning electron microscopy, FIB-SEM, FIB biological sample, FIB characterization

## 1. Introduction

With the evolution in science and technology, the need for latest equipment is getting powered up with every passing day. At first, the light microscopes were employed to watch micro objects which naked human eye cannot see. Later, with the need for higher resolution imaging instruments, electron microscopes were introduced, which gave much clearer and highly resolved 2D images [1–3]. Usually, stereological rules were used to produce 3D characteristics in micrographs of 2D sections [4–8]. This method of production, however, was not able to produce 3D images for objects with complex structures [9]. To be able to see the 3D models of even complex structures, many new techniques were introduced [10]. In the early stage, synchrotron and X-ray based tomographic techniques were introduced for 3D analysis of sample [11, 12]. Both of these are transmission techniques whereas the X-ray transmission technique uses the absorption difference between different phases of the samples and reconstructs a 3D image of the object [13]. Focused ion beam (FIB) is one of the 3D imaging techniques going head-to-head with confocal laser scanning microscopy (CLSM). The major difference between these two is that the CLSM uses LASER for scanning purposes whereas the FIB uses extremely focused [14–17].

The pioneering industry for FIB was mainly the semiconductor fabrication industry even till late 1980s [18–20]. But later, their applications for the characterizations of materials Introduced FIB's to materials and biological studies [21]. In material science studies, FIB helps in studying the material interfaces and their defects leading to failure and in biological sciences, it has mainly been used to study the interface between cells and tissues [22]. In start FIB's were single column and beam based instruments using energetic ion beam, of Gallium ion, for cross-section production into materials [19] followed by beam of secondary ions for producing images [23]. FIB uses a highly accelerated  $\text{Ga}^{3+}$  ion beam produced through liquid metal ion source (LIMS) with the energy ranging between 30 and 50 keV with beam diameter of around 5 nm [24].

FIB is basically a lithographic technique, offering very controlled and precise writing at micro and nanoscales [25] but when hyphenated with scanning electron microscopy (SEM) [26, 27], electron diffraction X-ray spectroscopy [28, 29], and transmission electron microscopy [30], it produces highly resolved 3D images. The FIB when hyphenated with EDS provides very accurate elemental analysis as well as very high-resolution images, but when hyphenated with the SEM, it produces very high-resolution and clean 3D images.

FIB-SEM hyphenation has been developed to produce 3D images by contrast means of SEM [20]. SEM-FIB uses dual beam mechanism to select the respective surface area of sample and images of the cross-sections of the selected area by milling [31]. Surface images are captured by SEM and scripting routine is followed for automatic performance [12]. The resolution of the produced 3D images depends totally upon the SEM resolution and the cutting precision of focused ion beam [12]. Highly resolved images in tens of nanometers resolution were produced by this technique, while to resolve further back scattered electrons is a good alternative [31]. Whereas, FIB-SEM connected with Energy Dispersive X-Ray Spectroscopy (EDS), gives very high resolution tomography with elemental analysis [28, 29]. Electron backscatter diffraction (EBSD) hyphenated with FIB-SEM gives information about grain size, defects, and grain boundary thickness [32], making it a very powerful tool.

The analysis of biological samples has always been a major issue due to its handling, stability, and the interaction of electron beam with the biological compounds present in the sample [33]. Since the biological samples are non-conductive, it is really hard to get high-resolution and accurate images [34]. Researchers in one of the methods have used sample drying at room temperature or mild heating. But in this method, changes in sample structure as well as the variation of chemical composition of the sample remain uncertain [35, 36]. The biggest improvement FIB-SEM has brought is the presence of primary and secondary columns sending an ion and electron beam simultaneously, resulting in coinciding milling and scanning [37]. This property adds majorly to the use of this technique for biological sample study at different resolutions and magnifications. It has also interested many researchers to look into cells and tissues ranging from single cell (prokaryotic and eukaryotic) to tissues and their interaction [1].

In this chapter, we will discuss the brief history and instrumentation of and developments in FIB. The application of hyphenated techniques like FIB-SEM, FIB-TEM, and FIB-SEM-EDS will be discussed from their analysis of material (at nanoscale) to biological samples (at microscale).

## **2. History and instrumentation**

The first ever field emission-based FIB was developed by Swanson and Orloff [38] and Levi-Setti [39] in 1975, which was based on gas field ionization sources (GFISs). The initial purpose of FIB was to repair and edit the circuits in

semiconductor industry [40, 41]. But nowadays, various ionization sources are available either commercially or as a prototype in research phase [42], advancing to the area of FIB for circuit modification in semiconductor industry to a characterization tool for materials as well as biological samples when connected with SEM [43]. The currently available FIBs are usually equipped with liquid metal ion sources, terming it to be LMIS-FIB tomography. These LIM sources have an edge over the previous ion sources for being more stable and capable of producing beams with long life time and low melting point, giving rise to high-energy ion sources with energy at much lower temperature [42]. Gas field ionization sources (GFISs), which use  $H^+$  ions which can reach lines lower than 10 nm, are also being used [44]. The tomographical aspects of FIB are enhanced when hyphenated with SEM. FEI was the first company to launch FIB/SEM Dual beam setup in 1993 [45]. The angle between ion and electron beams with reference to sample stage was in the range of  $10-82^\circ$ . The working principle of FIB and SEM is about the same with the only difference of beam source. In the case of SEM, a very well-focused electron beam is used whereas in the case of FIB, a highly accelerated ion beam is used to do the work. The ion beam is used to slice the selected area whereas the SEM scans the sliced sample simultaneously [46]. **Figure 1** (H1 and H2) (Adopted from Wierzbicki et al. [47]) shows the sliced 3 T3 fibroblast cell. 3 T3 is a living cell that produces collagen and extra cellular matrix [47]. **Figure 1** shows the unprocessed image of 3 T3 cell, **Figure 1** (H1) shows corrected top view on XZ-axis, and **Figure 1** (H2) shows corrected top view on XY-axis.

The electron beam in SEM is generated from an electron source which is usually W-wire or a lanthanum hexabromide tip. When the highly focused beam of electrons strikes the sample, it knocks out a low-energy electron from atomic orbital, called secondary electron (SE1), giving rise to a vacancy which is filled by a higher energy electron of the same atom. This results in release of an X-ray; the energy released in the form of X-ray is fingerprint energy of the element whose electron is knocked out. This X-ray helps to study the chemistry of the sample. An X-ray detector, usually EDS (energy dispersive X-ray spectrometer), is used for this purpose. Some primary electrons get in contact with the nuclei of the atom, which are then reflected back into the environment, called backscattered electron, whereas some of these electrons while being reflected back into the environment knock out an electron, giving out a secondary electron called secondary electron 2 (SE2). All these electrons being emitted contain specific information about the sample depending upon their origination site; for instance, SE1 contains high-resolution topographical information and originates at closer distance from the point of impact of electron beam, whereas SE2 originates from deep within the sample and is reflected at higher angle than SE1 and contains low-resolution topographical information about the sample. The SE1 generated from the sample surface is attracted by the electron detector which has a positively charged window on it, to gather the emitted electrons from all directions; these collected electrons are then amplified and their result is recorded. The electron beam raster scans the sample surface, giving rise to raster image. In SEM, the electrons generated in vacuum are attracted by a cathode, from where they get focused from a condenser lens. From the CL, this beam passes through magnetic lens which accelerates the electron which then passes through a deflection coil. The duty of this coil is to deflect the beam at any selected angle onto the sample. Then there is the last lens that focuses the beam onto the sample surface. There is a backscattered electron detector at the vent, which catches the backscattered electrons; these electrons give information about the chemical composition and crystal structure of the sample [46].

In the case of FIB, the previously used source for ions was the thermionic electron ion gun (TEIG) which released ions when heated at high temperature, whereas recently, FIBs use the field emission ion guns (FEIGs), in which electric field is



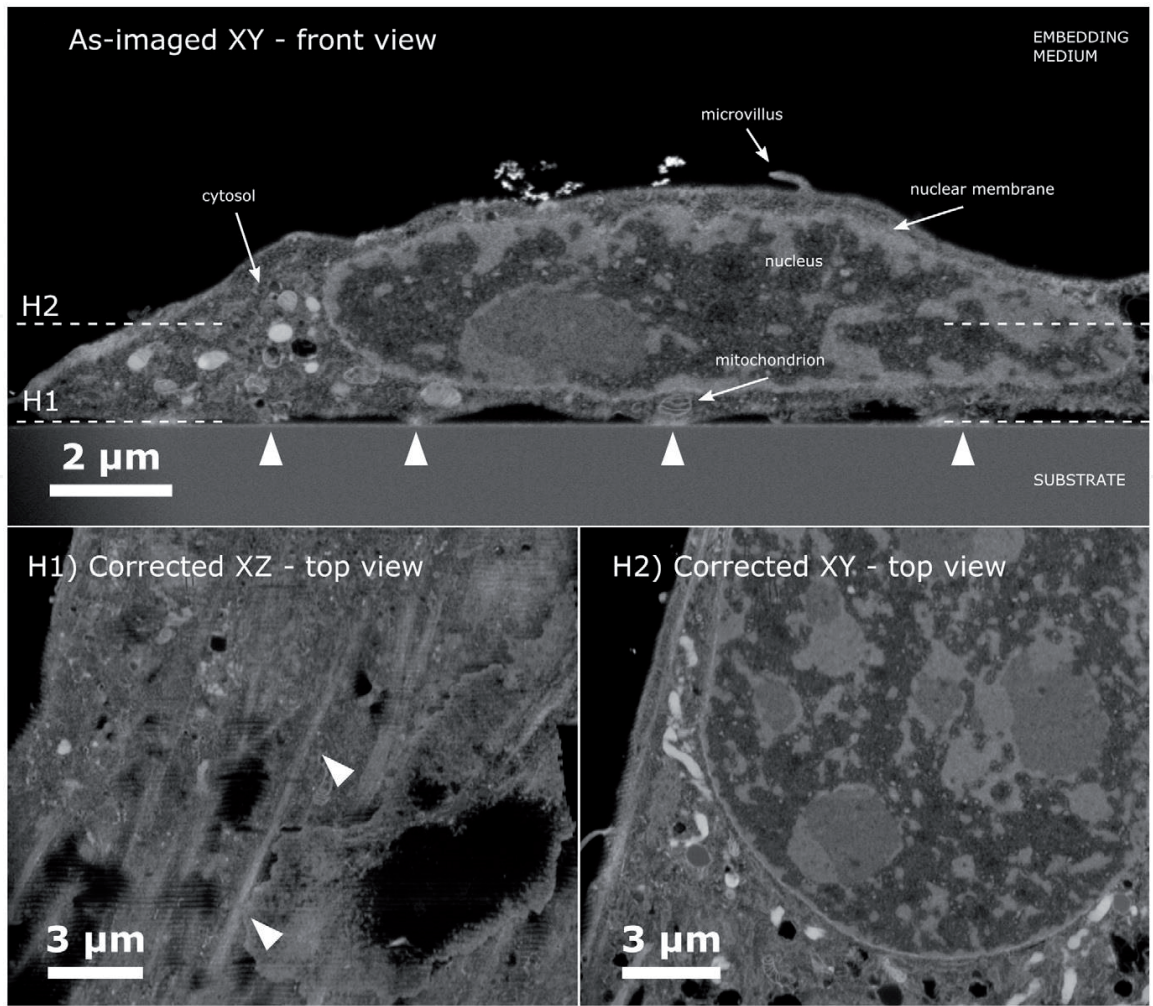


**Figure 1.**  
*Unprocessed image of 3 T3 cell, (H1) shows corrected top view on XZ-axis, and (H2) shows corrected top view on XY-axis.*

applied to get the ions from the source. The electrons are then focused by the help of a lens and pass through the scan coil, known as deflection coil, which focuses them onto the surface. This interaction of ion beam results in emission of ions (–ve or + ve charged species) and neutral atoms, by sputtering minute sections of the sample. The ion detector catches the ions and makes up the image of the sample. Besides the ejection of ions and neutral atoms, the ionic beam also knocks out some secondary electrons. The main reason of using the ion beam is the energy difference and impact diameter difference of the beam. For instance, the  $\text{He}^+$  beam is almost  $7600\times$  energetic than that of an electron beam and its wavelength is around  $100\times$  than electron beam used in SEM [48]; so this beam can easily reach sub 10-nm spot size [49].

Now when these two techniques are combined, they give very high-resolution images. If we compare SEM with FIB, the number of SE2's distort the resolution of SEM image, whereas in case of FIB, the backscattering is minimal, resulting in ejection of secondary electrons from the monolayer of sample, in turn resulting in very high-resolution image with versatile contrast in between deep and high points of the sample.

### 3. Materials characterization

#### 3.1 Materials

FIB/SEM is one of the latest tools for characterizing materials ranging from micro to nanometer scale. Due to the dual beam setup, FIB/SEM is one of the most

modern setups that use ion beam for slicing the sample and SEM for scanning purposes. Same goes for FIB-TEM and FIB-EDS characterization techniques, where FIB is a slicing/milling source whereas the TEM or EDS is a tool for respective characterization. In this section, we will explore the sample preparation and characterization method for various materials.

### *3.1.1 Sample preparation*

Multiple elemental reinforced alloys of composite material Al-Si were run through the FIB-SEM and FIB-EDS. The morphological arrangement of these samples depends upon the percentage of Si content present in the composite, the concentration of reinforcements as well as molding procedure [12, 50]. Reinforcements include Ni, Fe, and Mg. All the materials were grinded with the help of SiC paper at rotational speed of 300 rpm whereas SiC sizes were 320, 500, 1000, and 2400. Furthermore, the sample surfaces were worked with 1, 3 and 6  $\mu\text{m}$  particle sized DP-diamond paste at the rotator speed of 150 rpm, to get as shiny and smooth surface as possible, and the final touches were done using MgO. Nickel material for this purpose was produced following sintering [51].

### *3.1.2 Methodology*

FEI strata DB235 Dual Beam Workstation was used to analyze the sample which used Gallium ion source (Ion Beam) for milling and electron beam (SEM) for scanning purposes, with the adjusted angle between IB and EB of  $52^\circ$ . The area of interest of the sample was selected using SEM and was coated with the protective layer of Pt with the incorporation of FIB-induced decomposition of precursor gas. This protective layer helps in getting better cuts during milling [52]. The trench (by milling process) was dug into the sample in such a way that there is no shadow of sample edges over the trench during the scanning of the sample. **Figure 2** shows the image of a cell (Adopted from Wierzbicki et al. [47]) with the shadow of trench onto cell and its corrected version [47]. Sub image A shows the shadow of trench onto cell in XY-axis whereas sub image B shows its corrected version. It is better to mill at the edge area, but it is only possible for samples with evenly balanced composition and structure; for other samples, it is suggested to impute the area of interest from the sample and bring it to the edge with the help of micromanipulator. Whereas, two additional trenches may be dug around the area of interest to avoid the deposition of sputtered sample [52, 53]. The milling is done using current beam of order 20 nA. The milling criteria depend upon the milling of number of cross-sections needed to get a clear 3D surface of the smallest possible particle [12].

The area should essentially be polished with the implication of low currents in pA range to polish the surfaces before analyzing the sample and once polished, the samples analyzed using SEM at various ranges of resolution to get the best morphological structures needed. For instance the sample of AlSi12 was analyzed using increments of 300 nm and for AlSi7Sr, increments of SEM used were 83 nm [29].

## **3.2 Applications**

### *3.2.1 FIB/SEM tomography of squeeze cast AlSi7Sr*

Examples show the AlSi7 alloy sample reinforced with Sr. and studied with the help of SEM at 5 keV. This method helps in production of about 250 scanning images, with the intersliced distance of 60 nm obtaining 15  $\mu\text{m}$  of samples in

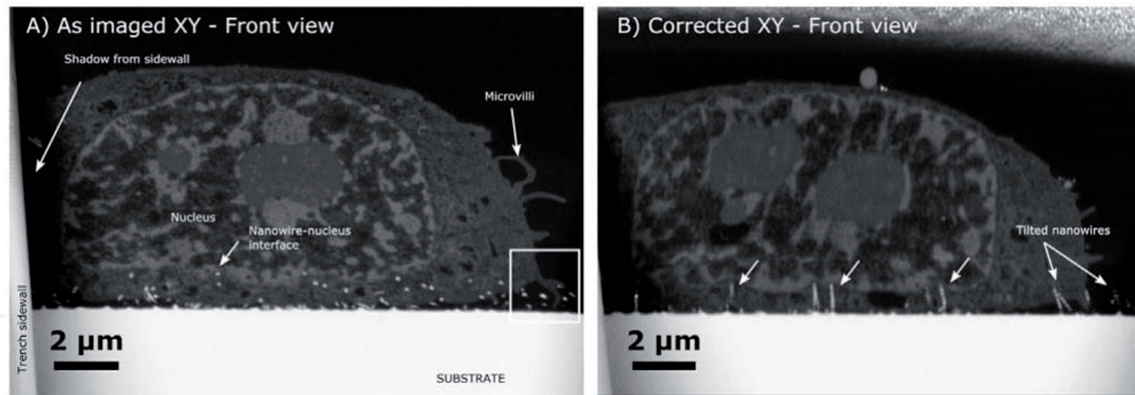


**Figure 2.**

*Image of a cell (Adopted from Wierzbicki et al. [47]). Sub image A shows the shadow of trench onto cell in XY-axis while sub image B shows its corrected version.*

milling direction. The Si in sample showed fibers and branches  $\sim 3\text{--}5\text{ }\mu\text{m}$  long with a diameter of  $200\text{--}500\text{ nm}$ . These fibers are intermingled and represented by difference of colors. The interconnection junction sizes were  $50\text{--}100\text{ nm}^2$ . The finally calculated volume fraction of Si in choral structure in reconstructed region was  $\sim 5\%$ .

### 3.2.2 FIB/SEM tomography of porous Ni

SEM high-voxel resolution helped in architecting the 3D structure of porous nickel, refer to paper [12] for assistance. 3D imaging revealed that around 2/3% volume of selected area was porous with totally interconnected structure. The canal internal caliber ranged from 500 to 2000 nm.

### 3.2.3 FIB/EDS tomography of squeeze cast AlSi12

FIB uses ion beam as working source, which is a result of interaction with sample producing the secondary electrons, but when equipped with energy dispersive spectrometer, this can help in determining the elemental composition of each milled slice [29, 31]. The use of EDS with FIB resulted in finding the elemental composition of AlSi12 sample with each slice's elemental data. When dealing with complex chemical structures, this new hyphenation technique proved to be worthy to produce data with each slicing and give exact chemistry of the compound of interest. As far as sample is concerned, the EDS used 8-keV acceleration to analyze each slice with the EDX (EDS) detector.

Results can be seen in [12].

## 4. Biological sample characterization

FIB-SEM is the most advanced technique to be used for the analysis of biological samples; to do so, several protective measures need to be taken, since biological samples are always sensitive to heat, moisture, and pressure. For this reason, the biological samples must be fixated, stained, and embedded in resin. Since biological samples are large, that is, microscale, they need a lot of time to get processed. Image processing time is the biggest limiting factor during biological sample running through the FIB-SEM, since the machine has to scan each block one by one to reconstruct a full 3D image. Therefore, there should a balance between sample scanning time and good resolution and suitable contrast. To reduce the time factor and enhance the resolution and contrast, new methods like chemical fixation,



high-pressure freezing, and freeze-substitution are being followed for sample preparation. **Figure 3** (Adopted from Wierzbicki et al. [47]) shows the interaction of Si nanowires with 3 T3 cell line. **Figure 3A** shows the nanowires taken up by the cell whereas **Figure 3B** shows the bending of nanowires under another cell [47].

#### 4.1 Chemical fixation treatment

Chemical fixation protocols use aldehyde fixation in the presence of uranyl acetate and osmium tetroxide by including thiocarbohydrazide osmium tetroxide [54] and tannic acid [34] (**Table 1**, adopted from [33]).

Currently, chemical fixation is the most widely used fixation technique among the researchers for FIB-SEM analysis of biological samples and high-resolution images can be recorded at a very small distance. At present, the large majority of FIB-SEM investigations are based on chemical fixation. For instance, animal liver tissue cell was examined under FIB-SEM and was fixated chemically with a chemical mixture of 2% OsO<sub>4</sub> modified with 1.5% K<sub>3</sub>Fe<sub>3</sub> + (CN)<sub>6</sub> and 20% glutaraldehyde for 120 min at room temperature in phosphate buffer. Extra staining was done with 2% uranyl acetate (aqueous) at room temperature.

#### 4.2 High-pressure freezing and freeze-substitution

Cryoimmobilization of samples for cryomicroscopy offers unique opportunities to inspect the sub-cellular structure in the absence of chemical fixation and metallic stains. Even though biological samples can be investigated under FIB-SEM for very clear images at room temperature [55], freeze substitution (FS) not only adds to the high conductivity of samples and high contrasting of images but also helps in preserving ultra-small structures when embedded with resin—because, during the FS processing, various desired chemicals and metallic agents can be put into the organic solvent to decrease the signal-to-noise ratio, resulting in the decline in the charging effect in FIB-SEM inspection of the samples.

Up until now, very few high-pressure freezing (HPF) and FS studies have been done for FIB-SEM sample preparation (**Table 2**, adopted from [33]). In one study [56], 24 different preparation protocols embracing HPF and FS techniques were used and no substantial difference was found in the contrast and structure of the cells. Another study did a comparative survey between the chemically and FS/HPF-fixated mouse liver cell samples, whereas, for TEM, a mixture of glutaraldehyde and

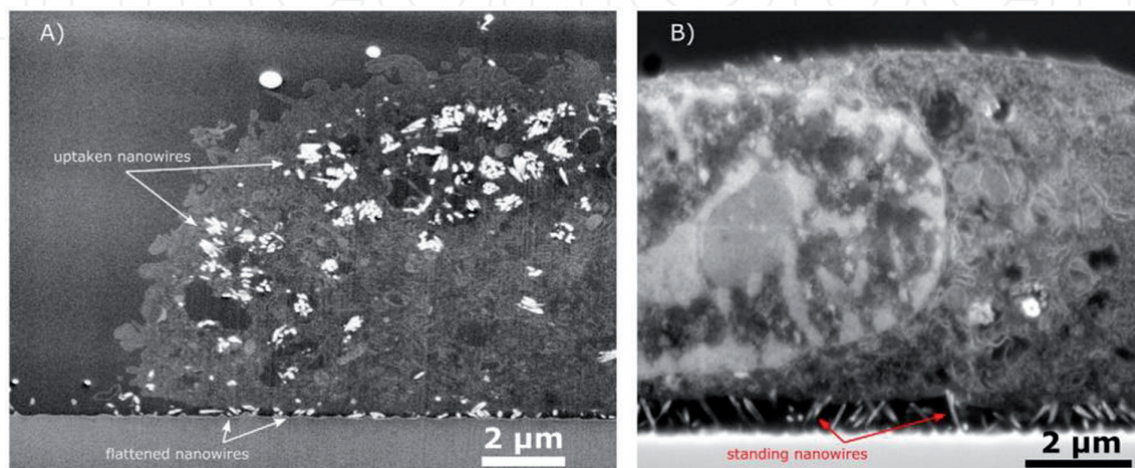


**Figure 3.**  
 (Adopted from Wierzbicki et al. [47]) shows the interaction of Si nanowires with 3 T3 cell line. **Figure 3A** shows the nanowires taken up by the cell whereas **Figure 3B** shows the bending of nanowires under another cell.



1. Reduced osmium with potassium ferro- or ferri-cyanide	2. Extended osmification with osmium-thiocarbohydrazide	3. Osmium tetroxide
Murphy et al. [56] Hekking et al. [58] Heymann et al. [59] Cretoiou et al. [60] Paredes-Santos et al. [61]	Murphy et al. [56] Leser et al. [62] Leser et al. [27] Felts et al. [63]	Heymann et al. [64] Murphy et al. [65] + <b>tannic acid</b> Bushby et al. [66] Armer et al. [67] Jimenez et al. [34] + <b>uranyl acetate</b> Murphy et al. [56] Leser et al. [62] Leser et al. [27] Merchán-Pérez et al. [55]

**Table 1.**  
*Variation in chemical fixation protocols described in the literature to perform FIB-SEM tomography of biological samples.*

1. OsO <sub>4</sub> + uranyl acetate + glutaraldehyde	Murphy et al. [56]
2. OsO <sub>4</sub> + uranyl acetate + H <sub>2</sub> O	Wei et al. [57] Villinger et al. [68]
3. Chemical pre-fixation following by HPF/FS in OsO <sub>4</sub> + uranyl acetate	Remis et al. [69]

**Table 2.**  
*Variation in freeze-substitution protocols described in the literature for FIB-SEM tomography on biological samples cryofixed by HPF.*

methy1 alcohol or acetone having hydrous or anhydrous uranyl acetate and OsO4 was used.

A study [57] has suggested that the difference in contrast between SEM and TEM images may be because of the fixatives, additive metals, and staining agents.

5. Conclusion

It is concluded that FIB-SEM, FIB-TEM, and FIB-EDS are the latest techniques currently being used for the characterization as well as the tomographic studies of materials and biological samples.

Acknowledgements

We are thankful to Dr. Ishaq Ahmed for inviting us to write this contribution to his edited book. We are also grateful to our research group for their help in writing up this chapter.

Furthermore, we are grateful to Dr. Kristian Molhave of DTU Nanolab, for giving us permission to adopt figures from his paper.

Conflict of interest

Authors have no conflict of interest.

IntechOpen

### Author details

Dilawar Hassan<sup>1</sup>, Sidra Amin<sup>1,3</sup>, Amber Rehana Solangi<sup>1\*</sup> and Saima Q. Memon<sup>2</sup>

1 National Centre of Excellence in Analytical Chemistry, University of Sindh, Jamshoro, Pakistan

2 Dr. M. A Kazi Institute of Chemistry, University of Sindh, Jamshoro, Pakistan

3 Department of Chemistry, Shaheed Benazir Bhutto University, Sindh, Pakistan

\*Address all correspondence to: [ambersolangi@gmail.com](mailto:ambersolangi@gmail.com)

### IntechOpen

© 2019 The Author(s). Licensee IntechOpen. This chapter is distributed under the terms of the Creative Commons Attribution License (<http://creativecommons.org/licenses/by/3.0>), which permits unrestricted use, distribution, and reproduction in any medium, provided the original work is properly cited. 

## References

- [1] Uchic MD et al. Three-dimensional microstructural characterization using focused ion beam tomography. *MRS Bulletin*. 2007;**32**(5):408-416
- [2] Franzini-Armstrong C. Electron microscopy: From 2D to 3D images with special reference to muscle. *European Journal of Translational Myology*. 2015;**25**(1):4836-4836
- [3] Rochow TG, Tucker PA. A brief history of microscopy. In: Rochow TG, Tucker PA, editors. *Introduction to Microscopy by Means of Light, Electrons, X Rays, or Acoustics*. Boston, MA: Springer US; 1994. pp. 1-21
- [4] Everett RK, Chu JH. Modeling of non-uniform composite microstructures. *Journal of Composite Materials*. 1993;**27**(11):1128-1144
- [5] Pyrz R. Quantitative description of the microstructure of composites. Part I: Morphology of unidirectional composite systems. *Composites Science and Technology*. 1994;**50**(2):197-208
- [6] Xi Y. Analysis of internal structures of composite materials by second-order property of mosaic patterns. *Materials Characterization*. 1996;**36**(1):11-25
- [7] Ghosh S, Nowak Z, Lee K. Quantitative characterization and modeling of composite microstructures by Voronoi cells. *Acta Materialia*. 1997;**45**(6):2215-2234
- [8] Howell PGT. *Stereological methods vol. 2: Theoretical foundation*: By E. R. Weibel academic press Inc., London, 1980 340 pages, many figures and tables ISBN 0-12-742202-1. *Scanning*. 1981;**4**(4):208-208
- [9] Webster R. Statistical analysis of microstructures in materials science. *European Journal of Soil Science*. 2001;**52**(3):527-527
- [10] Narayan RJ. Introduction. In: Narayan R, editor. *Rapid Prototyping of Biomaterials*. Sawston, Cambridge, United Kingdom: Horwood Publishing Limited; 2014. pp. xix-xxi
- [11] Maire E et al. On the application of X-ray microtomography in the field of materials science. *Advanced Engineering Materials*. 2001;**3**(8):539-546
- [12] Lasagni F et al. 3D Nano-Characterisation of Materials by FIB-SO/EDS Tomography. In: 11th European Workshop on Modern Developments and Applications in Microbeam Analysis. Bristol, United Kingdom: Institute of Physics; Vol. 72010. p. 012016
- [13] Baruchel J et al. Advances in synchrotron radiation microtomography. *Scripta Materialia*. 2006;**55**(1):41-46
- [14] Tata BVR, Raj B. Confocal laser scanning microscopy: Applications in material science and technology. *Bulletin of Materials Science*. 1998;**21**(4):263-278
- [15] Fritzsche C et al. Confocal laser scanning microscopy, a new In vivo diagnostic tool for schistosomiasis. *PLoS One*. 2012;**7**(4):e34869
- [16] Reyntjens S, Puers R. A review of focused ion beam applications in microsystem technology. *Journal of Micromechanics and Microengineering*. 2001;**11**(4):287-300
- [17] Friedensen S, Mlack JT, Drndić M. Materials analysis and focused ion beam nanofabrication of topological insulator Bi<sub>2</sub>Se<sub>3</sub>. *Scientific Reports*. 2017;**7**(1):13466
- [18] Nasrazadani S, Hassani S. Chapter 2 - modern analytical techniques in failure



analysis of aerospace, chemical, and oil and gas industries. In: Makhoulf ASH, Aliofkhazraei M, editors. *Handbook of Materials Failure Analysis with Case Studies from the Oil and Gas Industry*. Oxford, United Kingdom: Butterworth-Heinemann Publishing; 2016. pp. 39-54

[19] Moktadir Z. 14 - Graphene Nanoelectromechanics (NEMS). In: Skákalová V, Kaiser AB, editors. *Graphene*. Sawston, Cambridge, United Kingdom: Horwood Publishing Limited; 2014. pp. 341-362

[20] Xu CS et al. Enhanced FIB-SEM systems for large-volume 3D imaging. *eLife*. 2017;**6**:e25916

[21] Grandfield K, Engqvist H. Focused ion beam in the study of biomaterials and biological matter. *Advances in Materials Science and Engineering*. 2012;**2012**:6

[22] Santoro F et al. Revealing the cell-material interface with nanometer resolution by focused ion beam/scanning electron microscopy. *ACS Nano*. 2017;**11**(8):8320-8328

[23] Stevie FA. Focused ion beam secondary ion mass spectrometry (FIB-SIMS). In: Giannuzzi LA, Stevie FA, editors. *Introduction to Focused Ion Beams: Instrumentation, Theory, Techniques and Practice*. Boston, MA: Springer US; 2005. pp. 269-280

[24] Drobne D. 3D imaging of cells and tissues by focused ion beam/scanning electron microscopy (FIB/SEM). In: Sousa AA, Kruhlak MJ, editors. *Nanoimaging: Methods and Protocols*. Totowa, NJ: Humana Press; 2013. pp. 275-292

[25] Joshi-Imre A, Bauerdick S. Direct-write ion beam lithography. *Journal of Nanotechnology*. 2014;**2014**:26

[26] Drobne D et al. Surface damage induced by FIB milling and imaging

of biological samples is controllable. *Microscopy Research and Technique*. 2007;**70**(10):895-903

[27] LEŠER V et al. Comparison of different preparation methods of biological samples for FIB milling and SEM investigation. *Journal of Microscopy*. 2009;**233**(2):309-319

[28] Lasagni F et al. Three-dimensional characterization of 'as-cast' and solution-treated AlSi12(Sr) alloys by high-resolution FIB tomography. *Acta Materialia*. 2007;**55**(11):3875-3882

[29] Lasagni F et al. Three dimensional characterization of unmodified and Sr-modified Al-Si eutectics by FIB and FIB EDX tomography. *Advanced Engineering Materials*. 2006;**8**(8):719-723

[30] Bakhsh TA, Sadr A, Tagami J. Focused ion beam processing for transmission electron microscopy of composite/adhesive interfaces. *Journal of Adhesion Science and Technology*. 2015;**29**(3):232-243

[31] Schaffer M et al. Automated three-dimensional X-ray analysis using a dual-beam FIB. *Ultramicroscopy*. 2007;**107**(8):587-597

[32] Singh S et al. High resolution low kV EBSD of heavily deformed and nanocrystalline aluminium by dictionary-based indexing. *Scientific Reports*. 2018;**8**(1):10991-10991

[33] Kizilyaprak C et al. FIB-SEM tomography of biological samples: Explore the life in 3D. In: *Biological Field Emission Scanning Electron Microscopy*. 2019. pp. 545-566

[34] JIMÉNEZ N et al. Gridded Aclar: Preparation methods and use for correlative light and electron microscopy of cell monolayers, by TEM and FIB-SEM. *Journal of Microscopy*. Hoboken, New Jersey,

United States: John Wiley & Sons Ltd.; 2010;**237**(2):208-220

[35] YOUNG RJ et al. An application of scanned focused ion beam milling to studies on the internal morphology of small arthropods. *Journal of Microscopy*. 1993;**172**(1):81-88

[36] Braet F, De Zanger R, Wisse E. Drying cells for SEM, AFM and TEM by hexamethyldisilazane: A study on hepatic endothelial cells. *Journal of Microscopy*. 1997;**186**(1):84-87

[37] Taillon JA et al. Improving microstructural quantification in FIB/SEM nanotomography. *Ultramicroscopy*. 2018;**184**:24-38

[38] Orloff JH, Swanson LW. Study of a field-ionization source for microprobe applications. *Journal of Vacuum Science and Technology* 1975;**12**(6):1209-1213

[39] Levi-Setti R. Proton Scanning Microscopy: Feasibility and Promise. Chicago: IIT Research Institute; 1974. pp. 125-134

[40] Phaneuf MW. Applications of focused ion beam microscopy to materials science specimens. *Micron*. 1999;**30**(3):277-288

[41] Melngailis J. Focused ion beam technology and applications. *Journal of Vacuum Science & Technology, B: Microelectronics Processing and Phenomena*. 1987;**5**(2):469-495

[42] Bassim N, Scott K, Giannuzzi L. Recent advances in focused ion beam technology and applications. *MRS Bulletin*. 2014;**39**:317-325

[43] SCOTT K. 3D elemental and structural analysis of biological specimens using electrons and ions. *Journal of Microscopy*. 2011;**242**(1):86-93

[44] Lemme MC et al. Etching of graphene devices with a helium ion beam. *ACS Nano*. 2009;**3**(9):2674-2676

[45] Lindquist JM, Young RJ, Jaehnig MC. Recent advances in application of focused ion beam technology. *Microelectronic Engineering*. 1993;**21**(1):179-185

[46] Huang J, Cavanaugh T, Nur B. An introduction to SEM operational principles and geologic applications for shale hydrocarbon reservoirs; 2013. pp. 1-6

[47] Wierzbicki R et al. Mapping the complex morphology of cell interactions with nanowire substrates using FIB-SEM. *PLoS One*. 2013;**8**(1):e53307

[48] Joy D. SEM for the 21st Century: Scanning Ion Microscopy. Metallography, Microstructure, and Analysis. 2012;**1**:115-121

[49] Levi-Setti R. Proton scanning microscopy: Feasibility and promise. In: Johari O, editor. *Scanning Electron Microscopy, Part 1*. Chicago: IITRI; 1974. pp. 125-135

[50] Nafisi S, Ghomashchi R. Effects of modification during conventional and semi-solid metal processing of A356 Al-Si alloy. *Materials Science and Engineering A*. 2006;**415**(1):273-285

[51] Lasagni F et al. Nano-characterization of cast structures by FIB-tomography. *Advanced Engineering Materials*. 2008;**10**(1-2):62-66

[52] Holzer L et al. Three-dimensional analysis of porous BaTiO<sub>3</sub> ceramics using FIB nanotomography. *Journal of Microscopy*. 2004;**216**(1):84-95

[53] Holzer L, Cantoni M. Nanofabrication Using Focused ion and Electron Beams: Principles and Applications. *Review of FIB-Tomography*.

New York, NY, United States: Oxford University Press; 2012. pp. 410-435

[54] Tanaka K, Mitsushima A. A preparation method for observing intracellular structures by scanning electron microscopy. *Journal of Microscopy*. 1984;**133**:213-222

[55] Merchán-Pérez A et al. Counting synapses using FIB/SEM microscopy: A true revolution for ultrastructural volume reconstruction. *Frontiers in Neuroanatomy*. 2009;**3**:18

[56] Murphy G et al. Correlative 3D imaging of whole mammalian cells with light and electron microscopy. *Journal of Structural Biology*. 2011;**176**:268-278

[57] Wei D et al. High-resolution three-dimensional reconstruction of a whole yeast cell using focused-ion beam scanning electron microscopy. *BioTechniques*. 2012;**53**:41-48

[58] Hekking L et al. Focused ion beam-scanning electron microscope: Exploring large volumes of atherosclerotic tissue. *Journal of Microscopy*. 2009;**235**:336-347

[59] Heymann JAW et al. 3D imaging of mammalian cells with ion-abrasion scanning electron microscopy. *Journal of Structural Biology*. 2009;**166**:1-7

[60] Cretoiu D et al. FIB-SEM tomography of human skin telocytes and their extracellular vesicles. *Journal of Cellular and Molecular Medicine*. 2015;**19**:714-722

[61] Paredes-Santos T, de Souza W, Attias M. Dynamics and 3D organization of secretory organelles of *Toxoplasma gondii*. *Journal of Structural Biology*. 2011;**177**:420-430

[62] Leser V et al. Focused ion beam (FIB)/scanning electron microscopy

(SEM) in tissue structural research. *Protoplasma*. 2010;**246**:41-48

[63] L Felts R et al. 3D visualization of HIV transfer at the virological synapse between dendritic cells and T cells. *Proceedings of the National Academy of Sciences*. 2010;**107**:13336-13341

[64] Heymann JAW et al. Site-specific 3D imaging of cells and tissues with a dual beam microscope. *Journal of Structural Biology*. 2006;**155**:63-73

[65] Murphy G et al. Ion-abrasion scanning electron microscopy reveals distorted liver mitochondrial morphology in murine methylmalonic acidemia. *Journal of Structural Biology*. 2010;**171**:125-132

[66] J Bushby A et al. Imaging three-dimensional tissue architectures by focused ion beam scanning electron microscopy. *Nature Protocols*. 2011;**6**:845-858

[67] Armer H et al. Imaging transient blood vessel fusion events in zebrafish by correlative volume electron microscopy. *PLoS One*. 2009;**4**:e7716

[68] Read Villinger C et al. *Histochemistry and Cell Biology*. 2012;**138**:549-556

[69] Remis J et al. Bacterial social networks: Structure and composition of *Myxococcus xanthus* outer membrane vesicle chains. *Environmental Microbiology*. 2013;**16**:598-610